Supplementary Information for

"Crossover between Weak Antilocalization and Weak Localization of Bulk States in Ultrathin Bi_2Se_3 Films"

Huichao Wang[1,2], Haiwen Liu[1,2], Cui-Zu Chang[3,4], Huakun Zuo[5], Yanfei Zhao[1,2], Yi Sun[1,2], Zhengcai Xia[5], Ke He[2,3,4,*], Xucun Ma[2,3,4], X. C. Xie[1,2], Qi-Kun Xue[2,3] and Jian Wang[1,2,*]

[1]International Center for Quantum Materials, School of Physics, Peking University, Beijing 100871, People's Republic of China

[2]Collaborative Innovation Center of Quantum Matter, Beijing, People's Republic of China

[3]State Key Laboratory of Low-Dimensional Quantum Physics, Department of Physics, Tsinghua University, Beijing 100084, People's Republic of China

[4]Institute of Physics, Chinese Academy of Sciences, Beijing 100190, People's Republic of China

[5]Wuhan National High Magnetic Field Center, Huazhong University of Science and Technology, Wuhan 430074, People's Republic of China

* jianwangphysics@pku.edu.cn; kehe@iphy.ac.cn

I. Theoretical background

For the 5 quintuple layers Bi_2Se_3 topological insulator (TI) films, the surface states are weakly affected by the applied parallel magnetic field. For the parallel field magneto-resistance (MR) of the thin films, the main contribution is the phase factor $\exp\left(i\frac{e}{c\hbar}\int Adr\right)$ arising from the bulk states. The cooperon (particle-hole scattering diagram) in a system with strong spin-orbit coupling without magnetic field is [1,2]

$$C(q)=\frac{3}{2}\frac{1}{Dq^2+\frac{1}{\tau_\varphi}+\frac{2}{\tau_{SO}}}-\frac{1}{2}\frac{1}{Dq^2+\frac{1}{\tau_\varphi}}. \quad \text{(S1)}$$

Here, q is the momentum, D is the diffusion coefficient, τ_φ is the phase coherence time and τ_{SO} is the spin-flip time. By integrating all the cooperon terms, the correction to conductivity due to quantum interference is

$$\Delta\sigma = -\frac{2\sigma}{\pi\nu}C(r,r) = -\frac{2\sigma}{\pi\nu}\int\frac{d^2q}{(2\pi)^2}C(q)\,. \quad \text{(S2)}$$

In the above, σ is the conductivity and ν is the density of states. The mean free path l in the 5 quintuple layers Bi_2Se_3 film is about 20 nm, much larger than the thickness d=5 nm. In this approximately $l >> d$ limit, the diffusion equation for the cooperon in parallel magnetic field is given by

$$C(q) = \frac{3}{2}\frac{1}{Dq^2 + \frac{1}{\tau_B} + \frac{1}{\tau_\varphi} + \frac{2}{\tau_{SO}}} - \frac{1}{2}\frac{1}{Dq^2 + \frac{1}{\tau_B} + \frac{1}{\tau_\varphi}}\,. \quad \text{(S3)}$$

τ_B is defined by $\frac{1}{\tau_B} = \frac{1}{\tau}\frac{ld^3}{16L_B^4}$ where τ is the elastic scattering time and L_B is the magnetic length with $L_B = \sqrt{\frac{\hbar}{eB}}$. We define a characteristic time $\tau_1^{-1} = \tau_\varphi^{-1} + 2\tau_{SO}^{-1}$ and the corresponding length in this time scale is $L_{SO} = \sqrt{D\tau_1}$ where D is the diffusion coefficient. Then the correction to the conductivity is given by [1,2]

$$\Delta\sigma = -\mathrm{N}i\frac{e^2}{2\pi^2\hbar}\left[\frac{3}{2}\ln\left(1+\frac{ld^3}{16L_B^4}\frac{\tau_1}{\tau}\right) + \frac{1}{2}\ln\left(1+\frac{ld^3}{16L_B^4}\frac{\tau_\varphi}{\tau}\right)\right]. \quad \text{(S4)}$$

Here N_i is the number of energy bands contributing to the conductivity. By using the dephasing length $L_\varphi = \sqrt{D\tau_\varphi}$ and $L_{SO} = \sqrt{D\tau_1}$, we have the Equation (1) in the main text.

We introduce the detail calculation process for the parameters L_φ and L_{so} at 77 K when $B_{//}$ // I here. We assume the phase coherence length L_φ is dependent only on temperature thus $L_\varphi \approx 40$ nm at 77 K when $B_{//} \perp$ I. Moreover, considering the different effective spin-flip time τ_{SO} demonstrated by the anisotropic MR between $B_{//}$ // I and $B_{//} \perp$ I, we define and find a ratio of τ_{SO} ($B_{//}$ // I) / τ_{SO} ($B_{//} \perp$ I) from the 4.2 K fitting results. Utilizing the ratio and $L_{SO} \approx 18$ nm for $B_{//} \perp$ I at 77 K, $L_{SO} \approx 14$ nm for $B_{//}$ // I is deduced. The fitting curve utilizing $L_\varphi \approx 40$ nm and $L_{SO} \approx 14$ nm can quantitatively reproduce the MR behaviors at 77 K for $B_{//}$ // I configuration.

II. Transport properties of sample 2

Sample 2 is another 5 quintuple layers Bi_2Se_3 film on the sapphire (0001) substrate grown in the same MBE condition with sample 1. Similarly, 20 nm thick insulating amorphous Se is deposited on the film as capping layer for transport measurements. Figure S1(a) shows the sheet resistance-temperature characteristic of sample 2, which resembles that of sample 1 as shown in Fig. 2(a) of the main text. When applying a magnetic field perpendicular to the film plane, linear MR is observed at high fields, as shown in Fig. S1(b). In the parallel magnetic field, anisotropic MR behaviors along [110] direction are observed. With the increasing magnetic field when $B_{//} \perp I$ (Fig. S1(c)), the MR exhibits a switch from positive to negative at 4.2 K and 77 K with different switching fields, while only positive MR is observed within 50 T at both 4.2 K and 77 K when $B_{//} // I$ (Fig. S1(d)). These MR behaviors can be well explained by the WAL-WL crossover mechanism in TI bulk states as well. At the $B_{//} \perp I$ configuration, the MR switch at 4.2 K and 77 K corresponds to the crossover from WAL to WL. In the $B_{//} // I$ case, the positive MR indicates that only WAL is observed, which may be because the corresponding switching field from WAL to WL is larger than 50 T. Hall trace of sample 2, as shown in Fig. S2, reveals the sheet carrier density $n_s \sim 2.12\times10^{13}$ cm^{-2} and mobility $\mu \sim 245 cm^2/(V\cdot s)$ at 4.2 K. The tiny differences of transport properties between sample 1 and sample 2 may be caused by different sample qualities.

III. Control experiments

To have a comprehensive understanding of the WAL-WL crossover, control experiments for sample 1 are operated. As shown in Fig. S3, the MR behaviors, even the absolute values of the resistance, measured by 3 μA and 15 μA excitation current are identical, so are the MR data under opposite current direction. Current intensity and direction seem to count little for the MR behaviors.

We study the MR along [110] and [-110] directions by standard four-probe and quasi-four-probe method, respectively, thus the differences between the two measurement configurations are

further studied at 77 K with the same voltage distance in sample 1, as shown in the insets of Fig. S4. The MR change obtained by quasi-four-probe measurement is about 50% smaller than that measured by standard four-probe method, which may be because the former can introduce contact resistance and then reduce the negative MR amplitude.

Figure legends

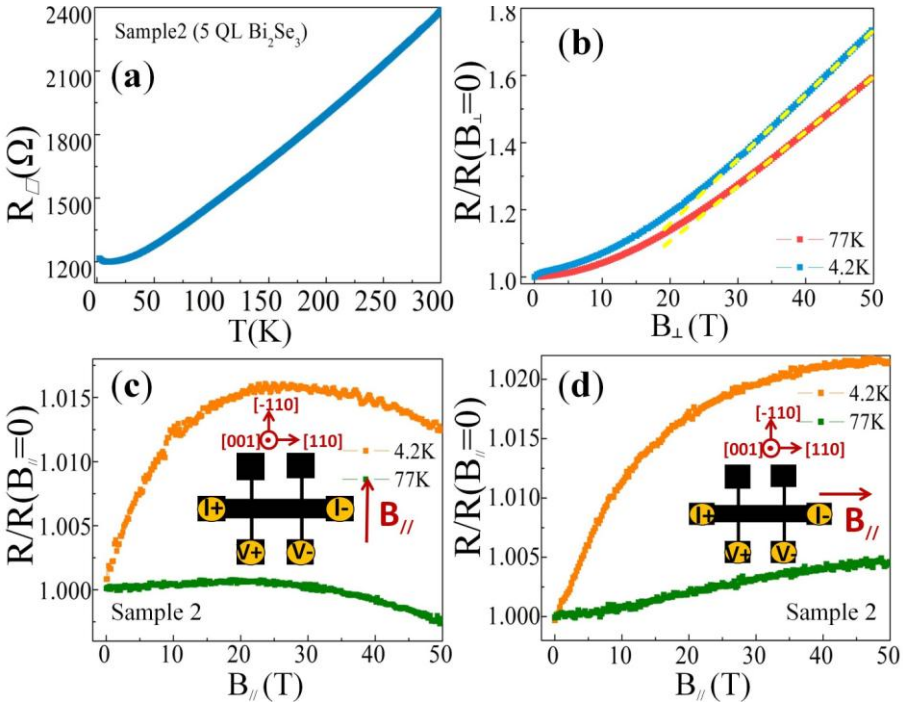

Figure S1 Transport properties of Sample 2. (a) Sheet resistance vs. temperature. Normalized magneto-resistance (b) in perpendicular field and at the configuration of (c) $B_{//} \perp I$ and (d) $B_{//} // I$. The black lines in (b) are guides to the eyes. The insets show the corresponding measurement schemas. (110) and (-110) mean two different crystal directions along the film plane. (001) means the crystal direction perpendicular to the film plane.

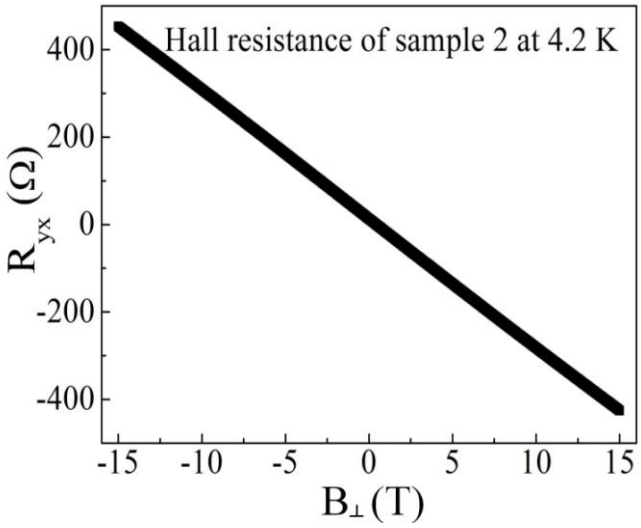

Figure S2 Hall resistance of sample 2 versus the perpendicular magnetic field at 4.2 K.

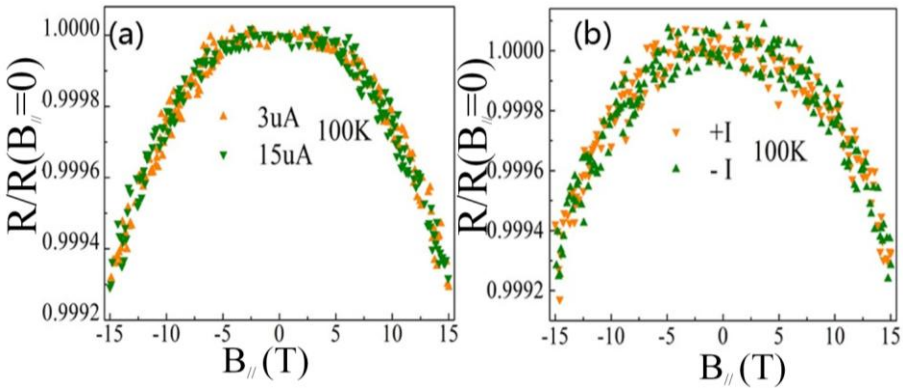

Figure S3 Normalized MR of sample 1 along [110] direction measured in parallel magnetic field with the excitation current of (a) 3 μA and 15 μA and (b) opposite directions.

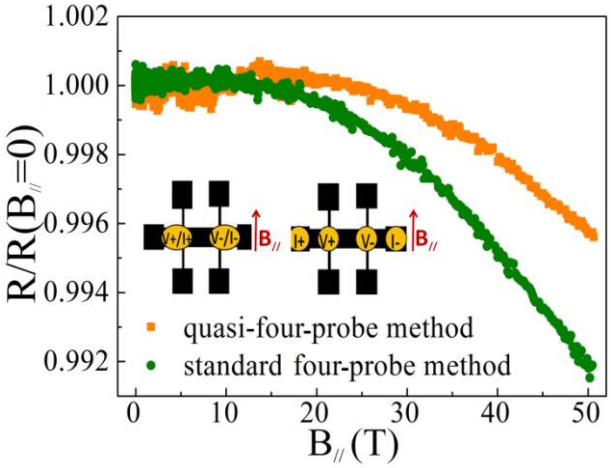

Figure S4 Differences of the measured parallel field MR results at 77 K between by standard four-probe and by quasi-four-probe method. The left and right insets show the measurement structures of the quasi-four-probe and standard four-probe method, respectively. The voltage distances between V+ and V- for two methods are same.

[1] B. L. Altshuler, A. G. Aronov, D. E. Khmelnitskii, and A. I. Larkin, *Quantum Theory of Solids*, edited by I. M. Lifshitz (Mir, Moscow, 1982), P. 130.

[2] V. K. Dugaev and D. E. Khmelnitskii, Sov. Phys. JETP 59, 1038 (1984).